

O. I. H. DIMITRY¹⁾, W. M. SAYED¹⁾, A. M. MAZROUA¹⁾, A. L. G. SAAD²⁾

Poly(vinyl chloride)/nanoclay nanocomposites — electrical and mechanical properties

Summary — Poly (vinyl chloride) (PVC) and dioctyl phthalate (DOP) plasticizer were mixed with small amounts (1–10 phr) of a layered silicate nanoclay consisting of 83.3 % of montmorillonite and 16.7 % of kaolinite to obtain PVC-based nanocomposites. The thermal stability of obtained products was characterized by thermal analysis using a thermogravimetric analyzer (TGA). The electrical conductivity of these composites was studied as a function of temperature and it was found that the activation energy for this property is lower than that of the host polymer. The composites exhibit increased Young's modulus and decreased Shore A hardness.

Key words: poly(vinylchloride), nanoclay, nanocomposites, thermal stability, electrical conductivity, mechanical properties.

NANOKOMPOZYTY POLI(CHLOREK WINYLU)/NANOGLINKA — WŁAŚCIWOŚCI MECHANICZNE I ELEKTRYCZNE

Streszczenie — Otrzymano nanokompozyty plastyfikowany poli(chlorek winylu)/nanoglinka (83,3 % montmorylonitu + 16,7 % kaolinitu) różniące się zawartością napełniacza (1–10 phr w przeliczeniu na PVC, tabela 1). Metodą TGA zbadano stabilność termiczną uzyskanych produktów, które do temp. 100 °C nie wykazują ubytku masy (rys. 1–3). Scharakteryzowano też ich właściwości dielektryczne (rys. 4 i 5) oraz zależność przewodności właściwej od zawartości nanoglinki i od temperatury (rys. 6–8, tabela 3). Na podstawie tej drugiej zależności obliczano energię aktywacji przewodnictwa nanokompozytów (tabela 3) stwierdzając, że są one pod tym względem zbliżone do półprzewodników. Zbadano też właściwości mechaniczne przy rozciąganiu oraz twardość omawianych produktów (tabela 4).

Słowa kluczowe: poli(chlorek winylu), nanoglinka, nanokompozyty, stabilność termiczna, przewodność właściwa, właściwości mechaniczne.

Polymer nanocomposites represent a new class of composite materials [1, 2] having improved properties at a much lower filler content — 3–5 wt. %, comparable to those obtained for 30–50 wt. % of micron-sized fillers [3]. The most successful results have been obtained using layered silicates as nanofiller precursors, and more especially with montmorillonite [4–7] (MMT), *i.e.* a mica-type silicate which consists of sheets arranged in a layered structure. It is used due to its large achievable surface area (about 750 m²/g) and its ability to swell [5]. The resulting nanocomposites show large improvements in barrier properties [8], flame resistance [9] and dimensional stability, as well as in mechanical properties such as tensile strength, tensile modulus and heat distortion temperature without a significant loss of optical transparence, toughness or impact strength [4, 10].

The literature contains numerous studies concerning polymer nanocomposites based on various polymer ma-

trices such as nylon 6, epoxy resin, polystyrene, polypropylene, polyethylene, poly (ethylene oxide), polyimide, poly (methyl methacrylate), polyurethane and others [11, 12]. In recent studies, little attention has been paid to poly(vinyl chloride) (PVC), which is frequently used as a suspension of fine particles in a liquid plasticizer.

Nanostructured conducting polymers have received much attention in the field of material sciences because of their unique mechanical and semiconducting properties and application in nano-materials and nanodevices. One of the main research and development domains is the fabrication of nanocomposites for the electronics industry as the rapid development of computers always demands the smaller components. Nano-technology operates with objects having particle sizes from below one up to hundreds nanometers [13].

This paper describes preparation of PVC-based nanocomposites filled with a layered silicate nanoclay and investigations of the effects of addition of small quantities of this nanofiller on the mechanical properties (Young's modulus, tensile strength, elongation and Shore A hardness) as well as electrical properties (permittivity, dielectric loss, and electrical conductivity) of plasticized PVC.

¹⁾ Egyptian Petroleum Research Institute, Petrochemical Department, Nasr City, Cairo, Egypt.

²⁾ National Research Center, Microwave Physics Department, Dokki, Cairo, Egypt.

EXPERIMENTAL

Materials

Layered silicate clay (Fayoum area, western desert of Egypt) consisting of 83.3 wt. % of montmorillonite and 16.7 wt. % of kaolinite was used as nanoclay. The X-ray diffraction analysis showed that nanocrystallites of the montmorillonite and kaolinite have a size of 15–20 nm.

The emulsion type of PVC (producer Petrochemicals Company at El-Ameria, Alexandria, Egypt; K -value — 70; apparent bulk density — 0.3 g/mL; viscosity number — 125 mL/g) was used as polymer matrix; dioctyl phthalate (DOP) served as PVC plasticizer and dibutyltin dilaurate — as a heat stabilizer.

Samples preparation

Several formulations were obtained by mixing of the components in the proportions shown in Table 1. Homogeneous samples were prepared by addition of the clay in variable proportions, at room temperature, under stirring, to a composition containing 100 parts of PVC and 100 parts of DOP. The mixtures were then mixed with 3 parts of dibutyltin dilaurate to give the required plastisols (gelation temperature at 175 °C for 100 s).

Table 1. Formulations of PVC-composites with variable proportions of nanoclay

Ingredients	Formulations, phr ^{*)}
PVC	100
DOP	100
Dibutyltin dilaurate	3
Clay	0, 1, 2, 3, 4, 5, 6, 7, 8, 9, 10

^{*)} Part per hundred parts of PVC.

Methods of testing

Thermogravimetric analysis (TGA)

Thermal stability of the prepared composites has been studied using a thermogravimetric analyzer (TGA). All TGA spectra were recorded under a nitrogen atmosphere at a temperature up to 600 °C using a program rate of 10 °C/min.

Dielectric measurements

The permittivity (ϵ') and dielectric loss (ϵ'') of the samples prepared were measured at different frequencies ranging from 100 Hz to 100 kHz. A LCR meter [type AG-4311 B, Ando electric unit (GM 45161/01, Philips, Netherland)] with the test cell NFM/5T [Wiss. Tech. Werkstätten (WTW) GMBH, Germany] was used. The capacitance C and loss tangent ($\tan \delta$) — from which ϵ' and ϵ'' were calculated — were obtained directly from the bridge. The samples were in the form of discs of

58 mm diameter and 3 mm thickness. Calibration of the apparatus was carried out using standard samples (Trolitul, glass and air) of 3 mm thickness; the accuracy of ϵ' was $\pm 1\%$ and of ϵ'' was $\pm 2\%$. The measurements were carried out at temperatures ranging from 30 to 100 °C using an ultrathermostat.

Electrical conductivity measurements

The electrical conductivity (σ) of the investigated samples was measured by the application of Ohm's law using the NFM/5T test cell. A power supply unit (GM 45161/01) from Philips (the Netherlands) was used. The potential difference V between the plates holding the samples and the current I flowing through it was measured using a multimeter (type URI 1050) from Rohde and Schwars (Germany). The electrical conductivity was calculated using the equation

$$\sigma = \frac{d \cdot I}{A \cdot V} \Omega^{-1} m^{-1} \quad (1)$$

where: d — is the thickness of the sample in meters and A is its surface area in square meters.

Mechanical measurements

Tensile strength, elongation, and Young's modulus were measured using a universal testing machine (model 3000, Shomatzo Company, Japan) at 23 ± 2 °C with a crosshead speed of 100 mm/min, a chart speed of 200 mm/min and a load cell range of 0–500 newton full scale according to ASTM D 638. 77a [13]. The dimensions of the sample were 3 mm thickness, 4 mm width, and 20 mm length. The mean value of five measurements for each sample was taken.

Shore A hardness was determined using a Shore A Durometer (model 306L ASTM produced by USA), according to DIN 53505 ASTM D2240 (1983). The Shore hardness value was taken as an average of five results at different points.

Morphology characterization

Phase morphology was studied using a Jeol JSM-T20 scanning electron microscope (SEM). For SEM observation the surface of the polymer was mounted on standard specimen stub. A thin coating ($\sim 10^{-6}$ m) of gold was deposited onto the polymer surface and attached to the stub prior to examination in the microscope to enhance the conductivity and secondary electron emission characteristic for the overgrowth.

RESULTS AND DISCUSSION

Thermal stability

TGA thermograms (Shimadzu-TGA-50H analyzer) of plasticized PVC and its composites show that they are stable with no weight loss up to 100 °C. The degradation of plasticized PVC (Fig. 1) and its composites containing 6 phr (Fig. 2) or 10 phr of clay (Fig. 3) starts above 100 °C

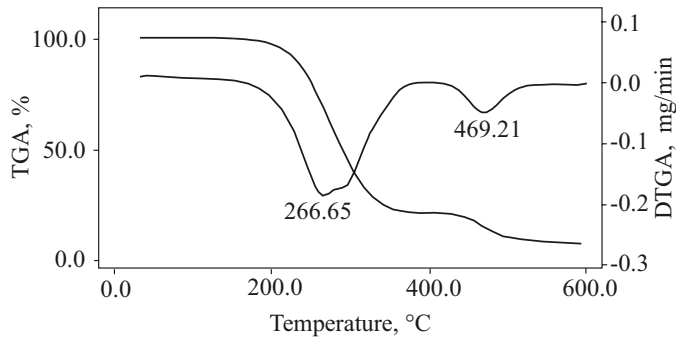


Fig. 1. TGA spectrum of plasticized PVC

and continues up to 469.21, 478.73, and 470.60 °C, respectively. At these temperatures, the percentages of degradation are 90.404, 86.177, and 88.792%, respectively. These data show that the largest delay in weight loss is observed for the composite containing 6 phr of clay which may be due to the fact that the dispersion of the clay platelets is better because the interfacial interaction between clay particles and PVC matrix, and that at higher filler content (10 phr), the thermal stabilization is less efficient, probably as a result of a less optimal platelets dispersion (sterical hindrance).

Electrical properties

Although polymer nanocomposites were found to enhance mechanical and thermal properties, their elec-

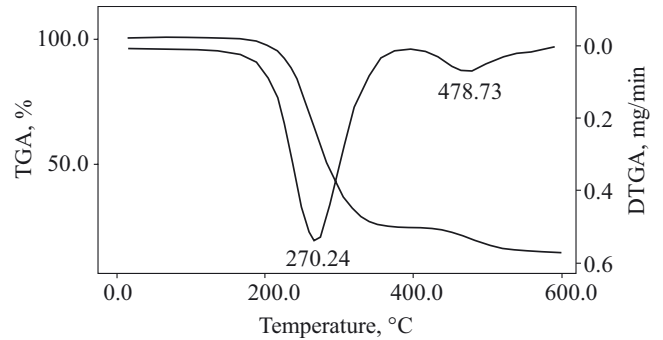


Fig. 2. TGA spectrum of nanocomposite PVC/6 phr of clay

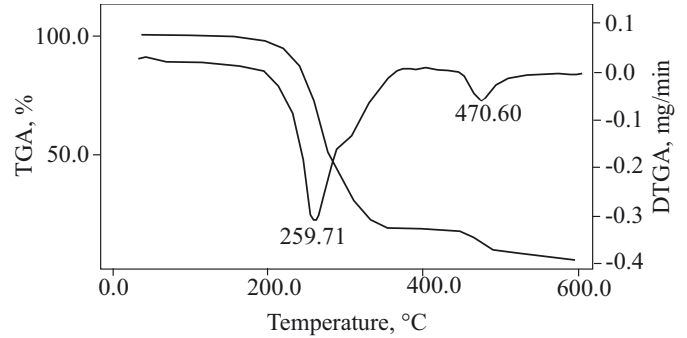


Fig. 3. TGA spectrum of nanocomposite PVC/10 phr of clay

trical properties have been ignored in the researches and the literature data in this subject are limited (there are only few of them) [14].

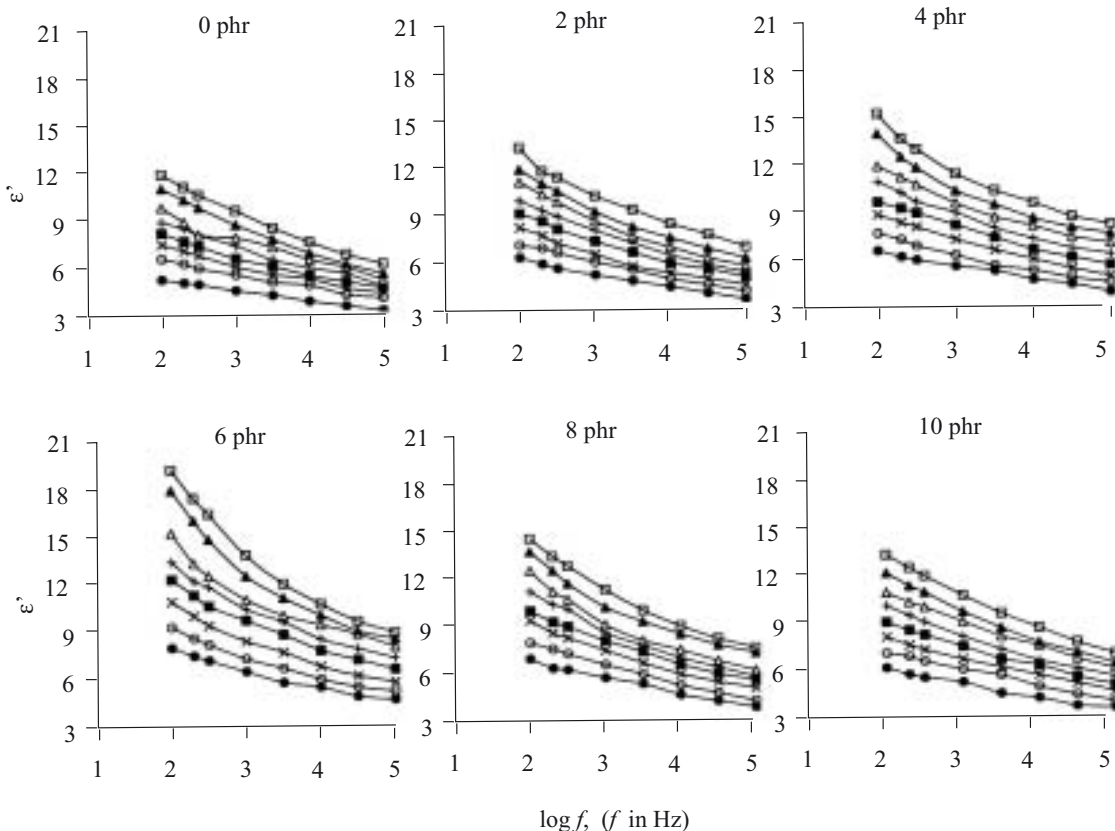


Fig. 4. Permittivity (ϵ') versus frequency (f) for PVC nanocomposites with variable proportions of nanoclay (0–10 phr) at different temperatures: • — 30 °C, o — 40 °C, x — 40 °C, ■ — 60 °C, + — 70 °C, Δ — 80 °C, ▲ — 90 °C, □ — 100 °C

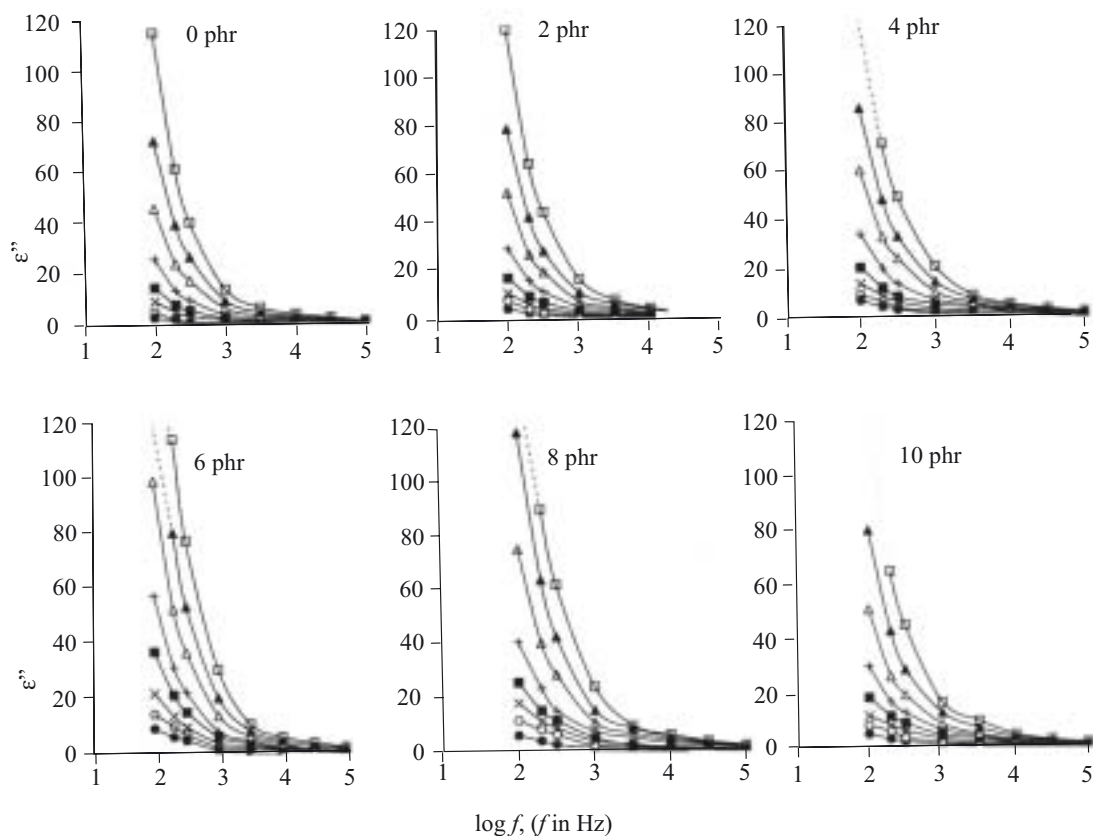


Fig. 5. Dielectric loss (ϵ'') versus frequency (f) for PVC nanocomposites with variable proportions of nanoclay (0–10 phr) at different temperatures: \bullet — 30 °C, \circ — 40 °C, \times — 40 °C, \blacksquare — 60 °C, $+$ — 70 °C, \triangle — 80 °C, \blacktriangle — 90 °C, \square — 100 °C

Dielectric characterization

As it was stated in Experimental Part, the ϵ' and ϵ'' values of the prepared composites have been investigated in the frequency region from 100 Hz to 100 kHz at temperatures 30–100 °C. It is evident from Fig. 4, which represents the variation of their ϵ' values versus frequency (f) at different temperatures, that ϵ' increases with increasing temperature and decreases with increasing frequency. Similar behavior was noticed before in the literature [15–19]. The increase in ϵ' with temperature can be explained by the increase in the mobility of polar groups, a decrease in density, and hence, a decrease in the effect of the environment that facilitates the orienta-

tion of the mobile groups. The decrease in ϵ' with frequency may be caused by dielectric dispersion.

From Fig. 5, which represents the variation of ϵ'' with frequency at different temperatures, it is apparent that the value of ϵ'' also increased at higher temperatures, especially rapidly in the lower frequency region. The low frequency losses are not totally dc-losses [20, 21] resulting from the increase in ion mobility but may comprise Maxwell–Wagner losses [22] resulting from an alternating current (ac) in phase with the applied potential, because the differences between the permittivities

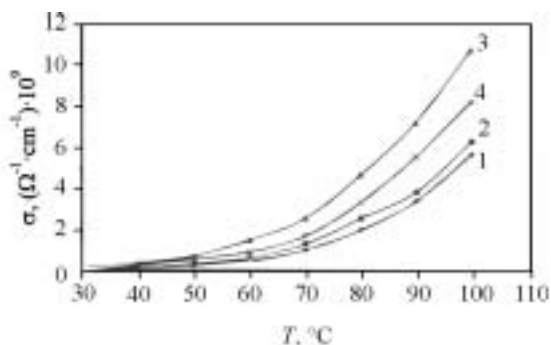


Fig. 6. Dependence of electrical conductivity (σ) on temperature (T) for PVC-nanocomposites with variable proportions of nanoclay; 1 — 0 phr, 2 — 4 phr, 3 — 6 phr, 4 — 8 phr

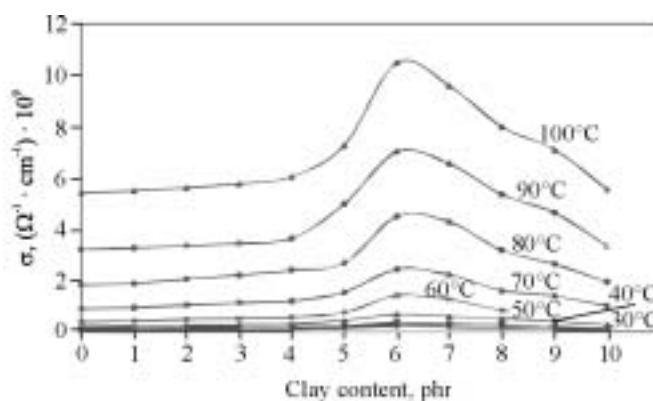


Fig. 7. Dependence of electrical conductivity (σ) on nanoclay content for PVC-nanocomposites with variable proportions of nanoclay (0–10 phr) at different temperatures

and conductivities of the different ingredients in the investigated samples are relatively large [17, 18].

Electrical conductivity

One of the interesting features of conductivity is its temperature dependence, which allows one to understand conduction mechanisms in the materials. Figure 6 shows such behavior of PVC and its composites with the clay under investigation. It is evident from this figure that the conductivity (σ) of all composites increases with increasing temperature due to the increase in the mobility of ionic bodies that takes place as a result of the excitation by heat. This characterizes semiconductor-like conduction in these composites.

Table 2. Electrical conductivity (σ) of PVC-composites with variable proportions of nanoclay

Samples ^{*)}	$\sigma \times 10^9$ ($\Omega^{-1} \text{ cm}^{-1}$) at temperatures ($^{\circ}\text{C}$)							
	30	40	50	60	70	80	90	100
PVC-0	0.05	0.10	0.22	0.41	0.92	1.85	3.23	5.46
PVC-1	0.08	0.13	0.26	0.45	0.96	1.90	3.29	5.54
PVC-2	0.09	0.15	0.27	0.50	1.06	2.07	3.36	5.65
PVC-3	0.09	0.16	0.29	0.53	1.14	2.22	3.47	5.80
PVC-4	0.11	0.18	0.32	0.58	1.21	2.41	3.66	6.07
PVC-5	0.15	0.24	0.46	0.77	1.55	2.70	5.01	7.30
PVC-6	0.23	0.38	0.69	1.42	2.45	4.52	7.04	10.48
PVC-7	0.20	0.32	0.61	1.28	2.23	4.30	6.57	9.59
PVC-8	0.14	0.28	0.53	0.84	1.60	3.19	5.38	8.00
PVC-9	0.11	0.22	0.43	0.75	1.40	2.64	4.65	7.12
PVC-10	0.08	0.14	0.28	0.54	1.01	1.94	3.34	5.57

^{*)} Samples symbols indicate the content of clay; for example PVC-4 means sample with 4 phr of clay.

Furthermore, Fig. 7, which represents the relation between conductivity and filler content at temperature from 30 to 100 $^{\circ}\text{C}$, and precise quantitatively the data presented in Table 2 show an increase in the value of σ of composites with increasing filler content up to 6 phr, especially at lower frequency region and higher temperatures. The obtained values are situated between the two extremes of those of semiconductors (10^{-10} — $10^{+2} \Omega^{-1} \text{ cm}^{-1}$) [23]. At still higher concentrations of the filler, the values of σ are decreased to some extent. This may be attributed to the formation of some nanoparticle agglomerates due to more intensive interfacial interactions between nanoparticles as further increase in the content of the filler may cause some steric hindrance that partially contributed to decreasing mobility of the electric charges.

In polymers, different conduction mechanisms are possible [24, 25]. Almost all mechanisms are related to different types of polarization taking place in the systems. Each of these mechanisms predominates in a given temperature range and applied electric field.

Activation energy for electrical conductivity

The activation energy (E) for electrical conductivity (σ) of PVC and its composites was calculated by plotting the logarithm of the conductivity *versus* the reciprocal of the absolute temperature (T) where a straight line was obtained, as shown for some examples in Fig. 8. The

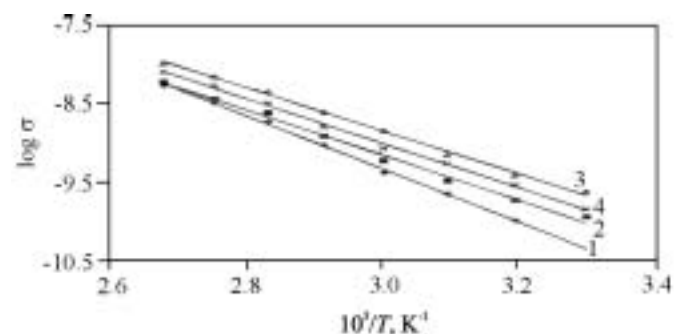


Fig. 8. Dependence of $\log(\sigma)$ on $10^3/T$ for PVC-nanocomposites with variable proportions of nanoclay; samples: 1 — PVC-0, 2 — PVC-4, 3 — PVC-6, 4 — PVC-8

results indicate, that PVC composites tend to behave as semiconductors. From the slope of the straight line, E was calculated using the equation [26]:

$$\sigma = \sigma_0 e^{-E/RT} \quad (2)$$

It has been found that the period of excitation depended on the activation energy needed to make the substance conducting. If the activation energy is low, *i.e.* the system is easily excited, the PVC composite becomes semiconducting at room temperature or in the presence of indirect light. Hence, it can be used for electronic devices working at ambient temperatures. It is apparent from Table 3 that the activation energy for electrical conductivity of plasticized PVC decreases with increasing concentration of the clay up to 6 phr. The lowest value of E for PVC-6 sample (5.28 Kcal/mol) indicates that it is easily excited and tends to behave as a semiconductor, so can be employed for electronic and microwave nano-devices.

Table 3. Activation energy (E) for electrical conductivity of PVC-composites with variable proportions of nanoclay

Samples ^{*)}	E , Kcal/mol
PVC-0	6.79
PVC-1	6.31
PVC-2	6.08
PVC-3	6.01
PVC-4	5.90
PVC-5	5.71
PVC-6	5.28
PVC-7	5.38
PVC-8	5.62
PVC-9	5.80
PVC-10	6.20

^{*)} See footnote under table 2.

Mechanical properties

The dependence of Young's modulus, tensile strength, elongation and hardness on the concentration of clay at 23 ± 2 °C is given in Table 4 (exact values) and represented in Fig. 9. The data show that increasing content of the clay from 1 to 10 phr causes increase in the

matrix due to lowering of their interfacial interactions between nanoparticles and matrix for 1 up to 10 phr loading of the clay. At 10 phr of nanoclay loading, the nanoparticles tend to interact together to form some particle agglomerates rather than to interact with PVC matrix what leads to poor interfacial adhesion between PVC and filler phase and to a subsequent retardation of

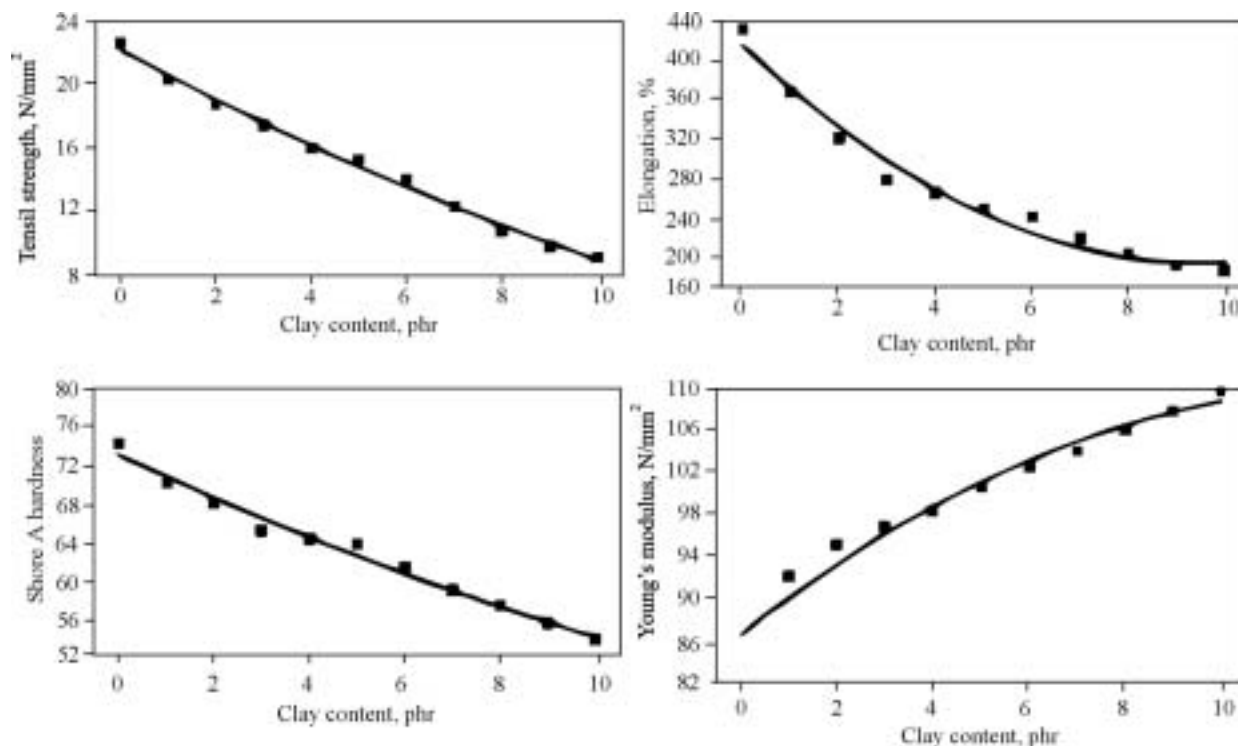


Fig. 9. Dependence of mechanical properties of PVC-nanocomposites on nanoclay content

value of Young's modulus as would be expected for high loadings of conventional mineral fillers. The presented data also show that tensile strength and elongation decrease with increasing filler content. The decrease in the tensile strength may be attributed to the decrease in the interfacial adhesion between the nanoparticles and PVC

crosslinks across the interfaces, and accordingly the tensile strength is largely decreased; but the composites still maintain good ductility. The decrease in elongation may be due to an interstructural process in which the filler molecules are distributed in the interaggregate space.

Table 4. Mechanical properties of PVC-composites with variable proportions of nanoclay

Samples ^{a)}	Tensile strength N/mm ²	Elongation %	Young's modulus N/mm ²	Shore A hardness
PVC-0	22.61	432.27	82.23	75.0
PVC-1	20.32	369.55	91.05	71.0
PVC-2	18.75	321.81	94.27	69.1
PVC-3	17.39	280.64	96.06	66.3
PVC-4	15.98	267.66	97.73	65.5
PVC-5	15.22	250.34	100.08	65.0
PVC-6	14.01	243.24	102.26	62.7
PVC-7	12.31	221.57	103.85	60.5
PVC-8	10.79	206.46	106.01	59.0
PVC-9	9.81	195.92	107.90	57.2
PVC-10	9.13	189.78	109.93	

^{a)} See footnote under table 2.

From the data presented in Table 4 and Fig. 9, it is also clear that Shore A hardness of PVC composites decreases with increasing clay content up to 10 phr.

Morphology

Figure 10 show SEM micrographs of pure PVC (a) and two samples of nanocomposites — PVC-6 (b) and PVC-10 (c). Figure 10b reveals that clay particles are dispersed homogeneously and no evidence of huge agglomerates is found. In opposite, when clay content is 10 wt. % the particles are very close surrounded by their "neighbors" and agglomerate formation occurred (Fig. 10c).

CONCLUSIONS

This study leads to the following conclusions:

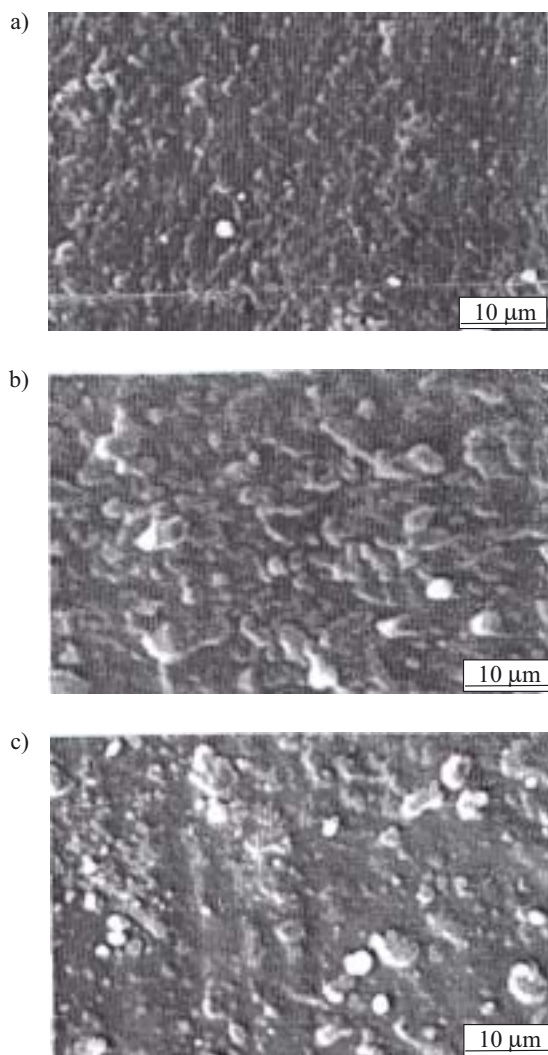


Fig. 10. SEM micrograph sample: PVC-0 (a), PVC-6 (b), PVC-10 (c)

— The addition of 6 phr of clay to PVC matrix increases its thermal stability which may be due to the dispersion of the clay platelets in PVC matrix.

— Electrical conductivity of PVC is enhanced for the addition of 6 phr of clay. The temperature dependence of the conductivity shows that the prepared composites are semiconductor-like.

— Activation energy for electrical conductivity is lowest for the composite containing 6 phr of clay, showing that it is easily excited and can be employed for electronic and microwave nanodevices as a semiconductor.

— With increasing content of nanoclay from 1 to 10 phr the value of Young's modulus increases as would be expected with high loading of conventional mineral fillers, and also some decrease in the tensile strength and

elongation are observed, but the nanocomposites still maintain good ductility.

REFERENCES

1. Fukushima Y., Inagaki S.: *J. Incl. Phenom.* 1987, **5**, 473.
2. Okada A., Kawasumi M., Kurauchi T., Kamigaito O.: *Polym. Prep.* 1987, **28**, 447.
3. Boucard S., Duchet J., Gerard J. F., Prele P., Gonzalez S.: *Macromol. Symp.* 2002, **194** (1), 241.
4. Alexandre M., Dubois P.: *Mat. Sci. Eng.* 2000, **28**, 1.
5. Pinnavaia T. J., Beall G. W.: "Polymer-Clay Nanocomposites", John Wiley and Sons, 2000.
6. Galeski A., Piorkowska E.: *Polimery* 2007, **52**, 323.
7. Olejniczak S., Kaźmierski S., Pallathadka P. K., Potrzebowski M. J.: *Polimery* 2007, **52**, 713.
8. Bharadwaj R. K.: *Macromolecules* 2001, **34**, 9189.
9. Beyer G.: *Fire Mat.* 2001, **25**, 193.
10. Berlund L.: *Filler Addit. Plast.* 2000, **4**, 31.
11. Jeziórska R., Klepka T., Pauksza D.: *Polimery* 2007, **52**, 294.
12. Zhang Y. H., Gong K. C.: *Mat. Res. Soc.* 1998, **520**, 191.
13. Leykin A., Ioelovich M., Figovsky O.: Eurofillers 2003 International Conference, Alicante (SPAIN) September 8-11 (2003), P363.
14. Dong X., Zhou G., Zhang J.: *Fangzhi Xuebao* 2004, **25** (4), 16.
15. Saad A. L. G., Hassan A. M., Gad E. A. M.: *J. Appl. Polym. Sci.* 1993, **49**, 1725.
16. Saad A. L. G., Hassan A. M., Youssif M. A., Ahmed M. G. M.: *J. Appl. Polym. Sci.* 1997, **65**, 27.
17. Saad A. L. G., Hussien L. I., Ahmed M. G. M., Hassan A. M.: *J. Appl. Polym. Sci.* 1998, **69**, 685.
18. Saad A. L. G., Sayed W. M., Ahmed M. G. M., Hassan A. M.: *J. Appl. Polym. Sci.* 1999, **73**, 2657.
19. Saad A. L. G., Aziz H. A., Dimitry O. I. H.: *J. Appl. Polym. Sci.* 2003, **91**, 1590.
20. Davies J. M., Miller R. F., Busse W. F.: *J. Am. Chem. Soc.* 1941, **63**, 361.
21. Sasabe H., Saito S. J.: *J. Polym. Sci., Part A: Polym. Chem.* 1969, **7**, 1405.
22. Hanna F. F., Yehia A. A., Abu Bakr A.: *Br. Polym. J.* 1973, **5**, 83.
23. Goodings E. P.: *Chem. Soc. Revs.* 1976, **5**, 95.
24. Kemeny G., Mahanti S. D.: *Proc. Nat. Acad. Sci. USA* 1975, **72**, 999.
25. Pochtennyi A. E., Ratnikov E. V.: *Dokl. Akad. Nauk BSSR* 1981, **25**, 896.
26. Eley D. D., Partfitt G. D.: *Trans. Faraday Soc.* 1955, **51**, 1529.

Received 28 X 2007.